Effect of C/A ratio on the crystallization behavior and structure of calcium-aluminate based alternative mold fluxes for casting medium and high Mn/Al steels

A Nigam[1], K. Biswas[2] and R. Sarkar[3]

[1]PhD Student, IIT Kanpur, Kanpur, Uttar Pradesh, India: 208016. Email: amann21@iitk.ac.in
[2]Professor, IIT Kanpur, Kanpur, Uttar Pradesh, India: 208016. Email: kbiswas@iitk.ac.in
[3]Assistant professor, IIT Kanpur, Kanpur, Uttar Pradesh, India: 208016. Email: rsarkar@iitk.ac.in

Keywords: Mould Fluxes, Continuous Casting, Advanced High-Strength Steels (AHSS), Clacium Aluminate, Differential Scanning Calorimetry (DSC), Raman Spectroscopy

ABSTRACT

Because of the problems with 1st and 2nd generations of Advanced High-Strength Steels (AHSS), a 3rd generation of AHSS steels has become prominent and these steels have properties in between the 1st and 2nd generations of AHSS. However, although the 3rd generation of AHSS is a promising candidate as a replacement for its predecessors, there remain some challenges in processing these

steels which are essentially medium Mn (Mn content ~ 5-7 wt.%) and high Al (Al content ~ 1-3 wt.%) steels. The use of conventional casting powders based on the $CaO-SiO_2$ system is unsuitable for high and medium Mn/Al steels. This work investigates the development of $CaO-Al_2O_3$-based mold fluxes for casting third-generation AHSS steel. Mold fluxes, with otherwise similar compositions but different C/A ratios, are tested, and their crystallization behavior is examined using Differential Scanning Calorimetry (DSC). A calcium aluminate phase having a composition $Ca_{12}Al_{14}O_{33}$ was found to be the main crystalline phase in the mold fluxes. A decrease in crystallization temperature was observed as the CaO/Al_2O_3 ratio increased from 1.00 to 1.33. The effective crystallization rate constant exhibited an increase with decreasing crystallization temperature, indicating a potential influence of nucleation rate on the overall crystallization rate and suggesting an anti-Arrhenius behavior in the crystallization process of these mold fluxes.

INTRODUCTION

Mold powders, either in granulated or non-granulated form, are introduced onto the top of liquid steel present within a copper mold. These mold powders generally have low melting point characteristics as their melting point lies usually below the pouring temperature of the liquid steel. Thus the superheat caused by the excessive temperature of the liquid steel helps the mold fluxes to undergo melting which creates a slag pool that infiltrates into the space between the solidifying steel shell and water-cooled copper mold. The primary role of these fluxes is to prevent the adhesion of the solidifying steel to the mold walls, ensuring efficient heat transfer and lubrication for the developing steel shell during solidification. The rapid cooling in the mold region results in the formation of a glassy slag film near the mold wall, which gradually transforms into a crystalline slag layer over time until reaching a stable state and near the shell region there will be liquid slag layer as shown in Figure 1. The solid part of the slag film governs the heat transfer because of its higher thermal conductivity and the liquid part helps in reducing the friction of the solidified steel shell which is moving down and thus will minimize the problems related to the surface quality of steels. Hence maintaining the thickness of the solid and liquid part of the slag film is important according to the type of steel being cast in the case of casting MC(medium carbon), peritectic steels, a thin, even shell is needed to avoid longitudinal and other surface cracking and this can be obtained with a low horizontal heat flux. Similarly in casting HC(high carbon) steels the shell is relatively weak and a thick shell is required to provide mechanical strength so a comparatively high heat flux is required. So for high horizontal heat flux thin slag film is required as heat flux is inversely proportional to thickness and vice versa for the low horizontal heat flux.

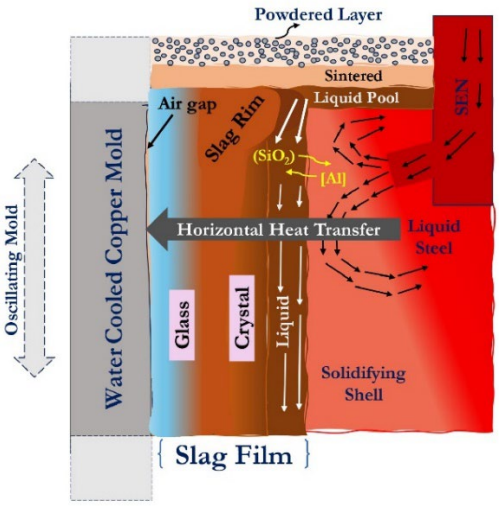

Interfacial Reactions

$3(SiO_2)+4[Al]=3[Si]+4(Al_2O_3)$

$3(MnO)+2[Al]=3[Mn]+2(Al_2O_3)$

FIG 1 – Schematic diagram illustrating the function of mold flux in the CC process

Typically, mold powders are calcium silicate-based, augmented with fluxing agents to tailor their properties for specific steel types. Conventional $CaO-SiO_2$ mold fluxes are commonly employed for casting low C steels with low Al and Mn content. However, the evolving steel industry, driven by demands for lighter steel in the automotive and aerospace sectors, has led to the development of 3rd Generation AHSS (Advanced High-Strength Steel) with higher Al (0.5-2 wt%) and Mn (5-7 wt%)

(Aydin *et al.*, 2013). While using the traditional CaO-SiO_2 based mold fluxes in casting 3rd Generation AHSS there are certain interfacial reactions like Equation 1(Kim and Park, 2012) involved between Al and Mn present in steel and SiO_2 present in the slag as Al and Mn has a more tendency to oxidize as they come below Si in the Ellingham Diagram. These interfacial reactions led to an increase in the Al_2O_3 content in the slag which led to an increase in the Al_2O_3/SiO_2 ratio of the slag by increasing the viscosity and melting temperature of the flux. This will create various surface defects in the cast steel like longitudinal cracks and break-out problems.

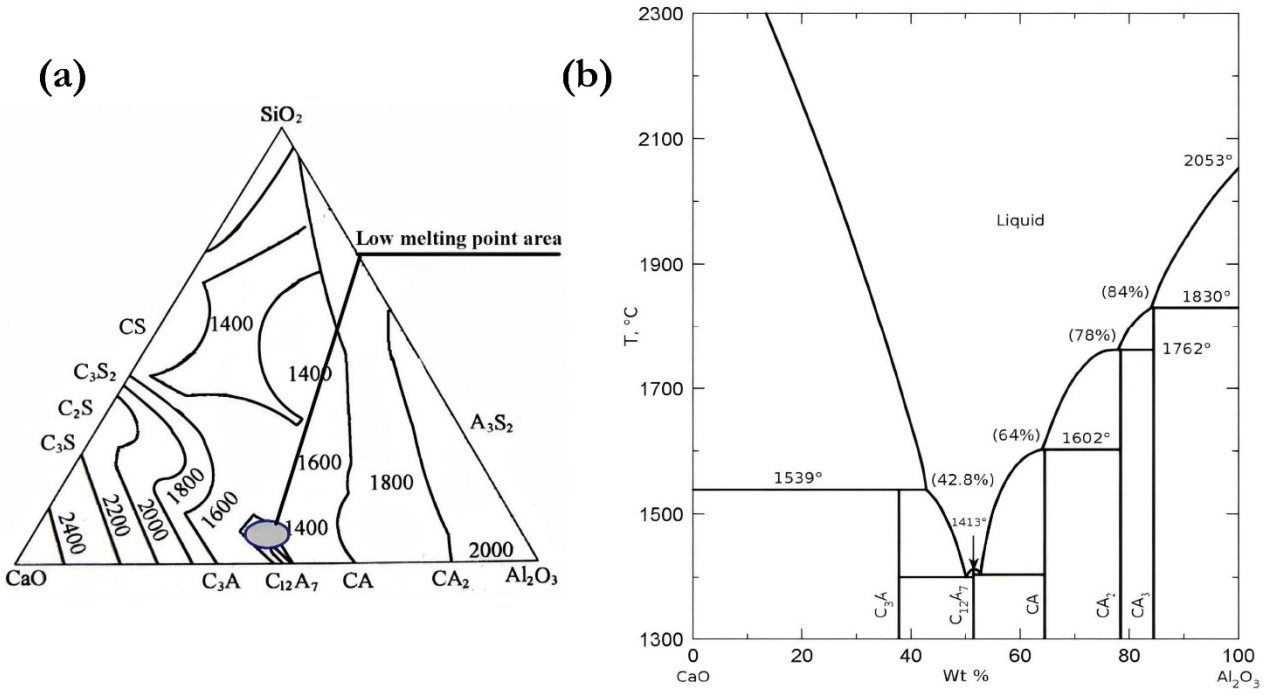

FIG 2 – (a) Liquidus projection of the SiO_2-CaO-Al_2O_3 system showing the low melting region (Liu *et al.*, 2014), (b) Binary phase diagram of CaO-Al_2O_3 showing the eutectic composition phase $C_{12}A_7$(Salasin and Rawn, 2017)

To address these challenges, there is a growing interest in using calcium aluminate-based mold fluxes, sometimes referred to as “Non-reactive” mold fluxes due to their minimal or absent silica content, eliminating interfacial reactions. Previous studies (Cho *et al.*, 2013; Zhang, Wang; and Shao, 2019) have found that lime-alumina-based mold fluxes exhibit physical characteristics similar to conventional fluxes, as long as the ratio wt%CaO/wt%Al_2O_3 remains close to 1.00. Furthermore, maintaining this wt%CaO/wt%Al_2O_3 ratio near 1.00 is crucial for ensuring that the fluxes have a low melting point because at that region low melting point phases lie, as depicted in Figure 2(a). The low melting point area in the ternary phase diagram depicts the formation of a line compound $C_{12}A_7$ phase as can be seen in the binary phase diagram of the CaO-Al_2O_3 system(Figure 2(b)) indicating that the $C_{12}A_7$ phase has a high melting point depression. So $C_{12}A_7$ phase can be incorporated into the mold flux system while designing the composition, as this phase formation will be quite useful to maintain the low crystallization temperature. Consequently, it is necessary to formulate these fluxes with a wt%CaO/wt%Al_2O_3 ratio near 1 and a SiO_2 content ranging from (3-6%) to minimize the interfacial reactions(Liu *et al.*, 2014). Also, by increasing the C/A ratio slightly greater than 1, an appropriate fraction of the primary crystalline phase i.e. may be achieved but this results in increasing the melting point of the flux. However, to reduce the melting point further fluxing agents like Na_2O, B_2O_3, CaF_2, and Li_2O are added to balance other thermophysical properties.

The crucial functions of mold fluxes—heat transfer and lubrication—are governed by the interfacial slag layer's resistance, particularly in horizontal heat transfer. This resistance is influenced by the fraction of crystal transformation (f_{crys}) as a function of temperature and time, which can be determined through methods such as confocal microscopy (CSLM) and DSC/DTA. Therefore, understanding the crystallization kinetics of the forming phases is essential for comprehending heat transfer.

In the present study, two compositions of calcium aluminate mold fluxes with varying CaO/Al_2O_3 ratios (1.00 and 1.33) were developed. Isothermal crystallization kinetics were investigated at different temperatures for both compositions, and various crystallization parameters were determined to characterize the type of crystallization mode and the activation energy involved in that crystallization phase.

EXPERIMENTAL DETAILS:

A. Sample Preparation:

Mold flux samples were prepared on a laboratory scale using reagent grade CaO, Al_2O_3, Na_2CO_3, CaF_2, SiO_2, and B_2O_3. Calcination of Na_2CO_3 to Na_2O was done by putting Na_2CO_3 at 800°C for 12 hours in an air environment in a muffle furnace. The powders were then thoroughly mixed with the help of acetone in a mortar and pestle and then kept in the oven for 2 hours at 100°C for the removal of moisture. Samples were then heated and melted in a graphite crucible inside a muffle furnace kept at 1400°C for 1 hour. Subsequently, the melted liquid flux was quenched in water, and glassy cullets were obtained which was verified through XRD as seen in Figure 3(a). These were then pulverized for further examination of the composition of the samples by XRF to determine whether there was any evaporation loss or not. Pulverized samples were then used in the DSC experiments to study the crystallization kinetics.

Sample(wt/wt)%	CaO	Al_2O_3	Na_2O	B_2O_3	CaF_2	SiO_2
CaO/Al_2O_3=1.00	35	35	15	5	5	5
CaO/Al_2O_3=1.33	40	30	15	5	5	5

TABLE 1 – Chemical composition of the mold flux (weight%)

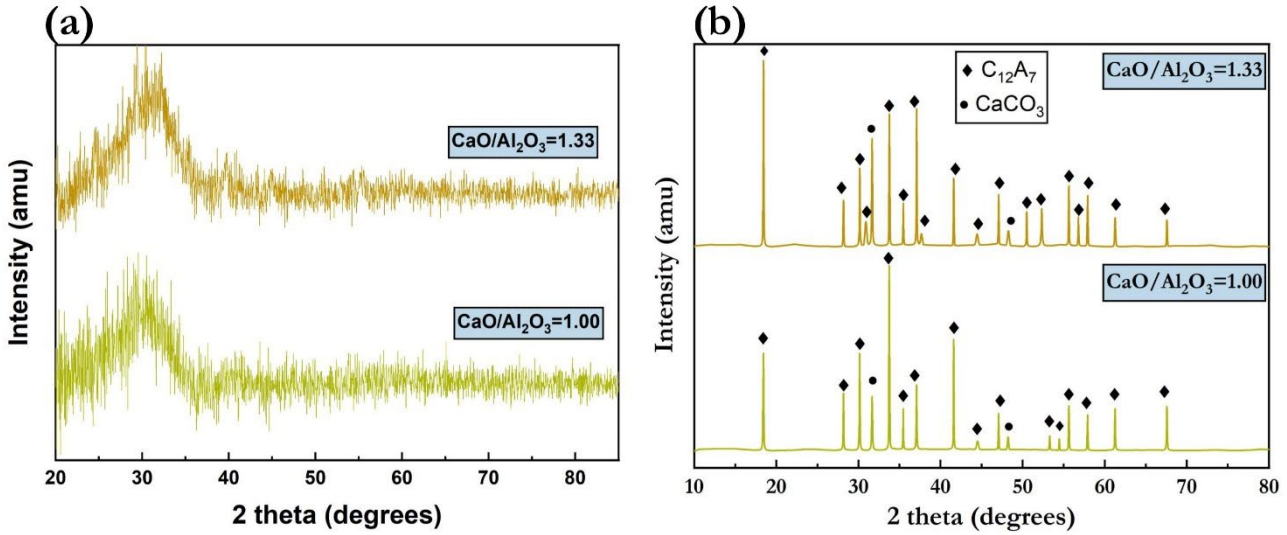

FIG 3–(a) XRD plot of the two compositions after quenching, (b) XRD plot of the two compositions for the crystallized sample

B. DSC Measurements:

The crystallization kinetics of the fluxes were evaluated isothermally at different temperature ranges with DSC (STA 2500 Regulus; NETZSCH Instrument Inc., Germany). Measurement of the samples was done in a platinum crucible with a lid under an N_2 atmosphere at a flow rate of 60 mL/min. For each experiment 50 to 60 mg of the pulverized samples were subjected to a thermal cycle (Seo *et al.*, 2015) as shown in Figure 4 under which the samples were heated at a constant rate of 25 K/min up to a target temperature (Tc) (determined by doing a normal DSC scan of the sample upto a temperature of 1400°C, Figure 5(a)) after which sample was isothermally held at that temperature

for 2 hours followed by subsequent cooling at a faster rate. After each experiment, samples were collected and examined in XRD and SEM-EDS for phase determination.

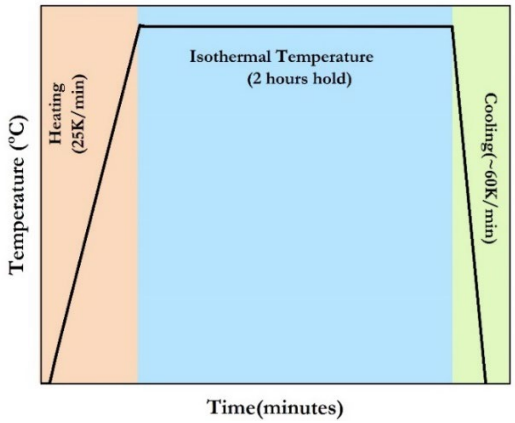

FIG 4– Thermal cycle for the isothermal experiments

Results and Discussions:

A. Isothermal DSC Measurement:

DSC experiments for two of the fluxes were carried out only after analyzing the crystallization temperature (T_c) through a normal DSC scan as seen in Figure 5. The crystallization temperature is the peak temperature of the crystallization event that occurred during the heating of the sample. Figure 5 shows the scans for the isothermal crystallization of the flux wt%CaO/wt%Al_2O_3 =1.00. There is only one peak of crystallization which was identified through XRD as $C_{12}A_7$ ($Ca_{12}Al_{14}O_{33}$) (Figure 3(b)). DSC experiments for wt%CaO/wt%Al_2O_3 =1.33 showed similar profiles.

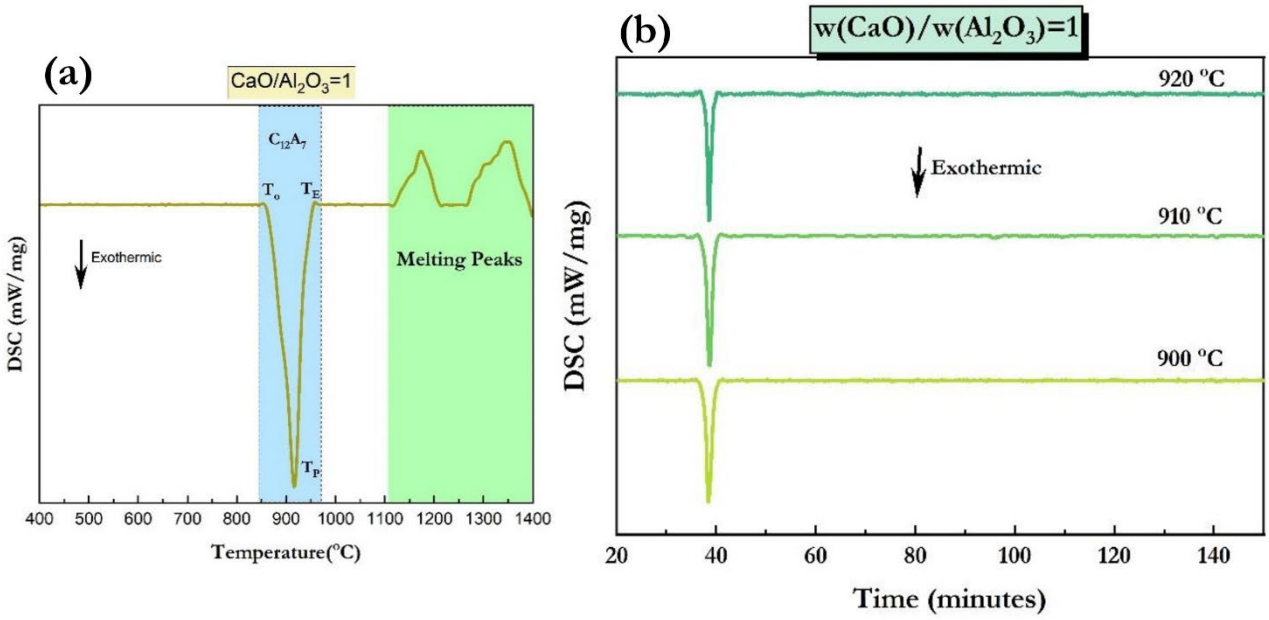

FIG 5–(a) DSC scan at 10 K/min for the identification of different peaks,(b) DSC scans for isothermal crystallization of CaO/Al_2O_3=1.00

B. Isothermal Melt Crystallization Kinetics:

Crystallization is an exothermic process as can be seen in the DSC scans(Seo *et al.*, 2015). As the rate of heat release is proportional to the rate of crystallization, the relative degree of crystallinity (α) can be obtained as:

$$\alpha(t) = \frac{\Delta Ht}{\Delta Htotal} = \frac{\int_0^t \left(\frac{dH_c}{dt}\right) dt}{\int_0^\infty \left(\frac{dHc}{dt}\right) dt}$$

where ΔH_t is the enthalpy as a function of the time from initial to a given crystallization time and ΔH_{total} is the total enthalpy reached at the end of the isothermal crystallization process. Figure 6 shows the relative degree of crystallinity as a function of crystallization time for CaO/Al_2O_3=1.00. So, we can say that the sigmoidal curve shifted towards the right with an increase in temperature indicating the overall crystallization rate $\left(\frac{d\alpha}{dt}\right)$ for $C_{12}A_7$ phase formation decreases with an increase in the crystallization temperature.

The isothermal crystallization kinetics of the flux can be understood with the help of the JMAK equation(Avrami, 1939)

$$\alpha(t) = 1 - \exp(-(kt)^n)$$

Where α(t) is the relative degree of crystallinity at time t (excluding incubation time),n is the Avrami exponent associated with the crystallization mode and k is the effective crystallization rate constant, which is dependent on temperature and rate of nucleation, and crystal growth. The values of n and k can be obtained by fitting the double logarithmic form as follows:

$$\ln\{-\ln[1-\alpha(t)]\} = n\ln k + n\ln t$$

The plots of $\ln\{-\ln[1-\alpha(t)]\}$ versus $ln\ t$ are also shown in Figure 6. From the slope and intercept the values of n and K can be obtained values of which are summarized in Table 2. The average value of n for CaO/Al_2O_3=1 lies around 4 and for CaO/Al_2O_3=1.33 value lies around 3.5. The crystallization parameters, calculated from isothermal crystallization experiments for both fluxes are reported in Table 2. It is noted from Table 2 that the values of effective crystallization rate constant k for both the fluxes increase with the decreasing crystallization temperature(T_c).

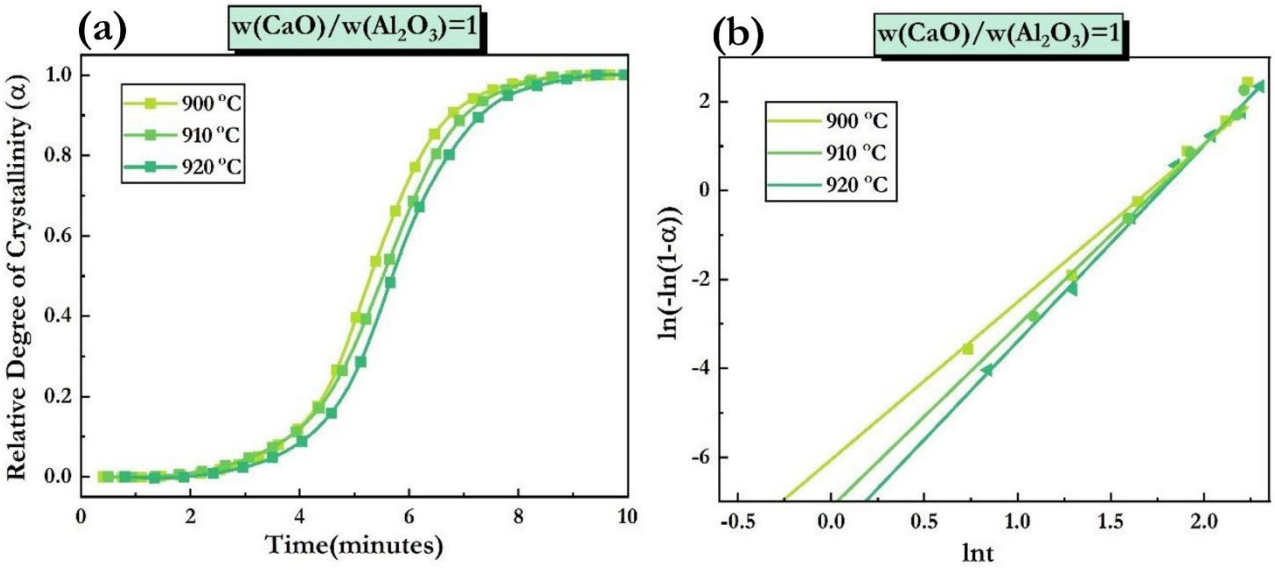

FIG 6– (a) Relative degree of Crystallinity(α) with time ,(b) $\ln\{-\ln[1-\alpha(t)]\}$ vs $\ln t$ plots for isothermal crystallization of CaO/Al_2O_3=1.00

Sample	**T_c (°C)**	**n**	**k (min^{-1})**
CaO/Al_2O_3=1.00	900	3.548	0.1813
	910	4.082	0.1747

	920	4.144	0.1519
CaO/Al_2O_3=1.33	790	2.701	0.2119
	800	3.136	0.1919
	810	4.272	0.1832

TABLE 2 – Results of the Avarami analysis for isothermal crystallization

The effective crystallization rate constant k can be used to determine the crystallization activation energy through the Arrhenius equation.

$$(\ln k) = \ln A - \frac{E}{RT_c}$$

Where A is the temperature-independent pre-exponential term, n is the Avrami exponent, E is the effective activation energy, R is the universal gas constant and Tc is the crystallization temperature. Figure 7 shows the plot of $(\ln k)$ versus $(1/T_c)$ for the isothermal crystallization of both mold fluxes. The effective activation energy determined from the slope of the plot for CaO/Al_2O_3=1 and1.33 is -102.75 KJ/mol and -69.72 KJ/mol, respectively. These values indicate that the mold flux melt crystallization may be controlled by the free energy change for nucleation related to the degree of undercooling. Activation energy represents the energy barrier that must be overcome for a reaction to occur. In the case of crystallization, nucleation is the initial step where small clusters of atoms or molecules come together to form a stable nucleus, which then grows into larger crystalline structures. Lower activation energy values, such as those obtained (-102.75 kJ/mol for CaO/Al_2O_3=1.00 and -69.72 kJ/mol for CaO/Al_2O_3=1.33), imply that the energy barrier for nucleation is lower. This means that it requires less energy for the nucleation process to initiate, making it more favorable and easier for nuclei to form. Undercooling refers to the extent to which a liquid is cooled below its equilibrium melting point before crystallization occurs. When undercooling is significant, nucleation becomes the rate-limiting step in the crystallization process because it is the initial barrier that must be overcome for crystals to form. Given the lower activation energy values observed, it suggests that the energy barrier for nucleation is relatively low, indicating that nucleation is more likely to occur even at lower degrees of undercooling. Therefore, nucleation is expected to be the dominant factor governing the overall crystallization rate for both mold fluxes, as it represents the crucial initial step in the crystallization process (Vyazovkin and Sbirrazzuoli, 2003; Papageorgiou *et al.*, 2005).

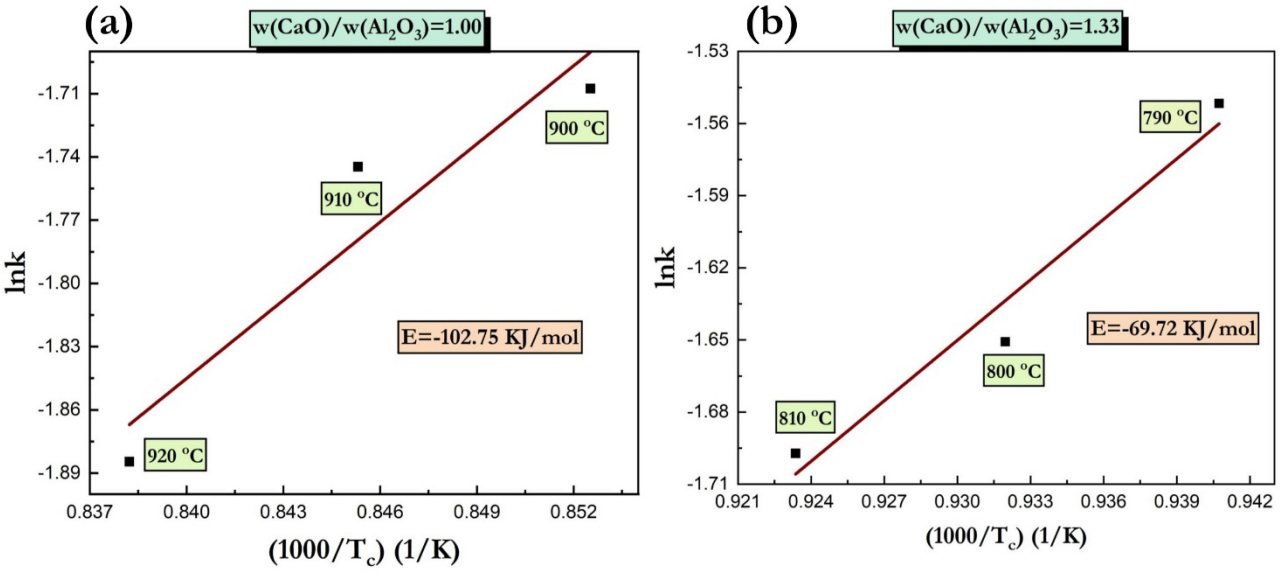

FIG 7– Plots of ($\ln k$) vs 1/T_c for isothermal crystallization of (a) CaO/Al_2O_3=1.00, (b) CaO/Al_2O_3=1.33

C. Structural Analysis of the $CaO\text{-}Al_2O_3$ based fluxes:

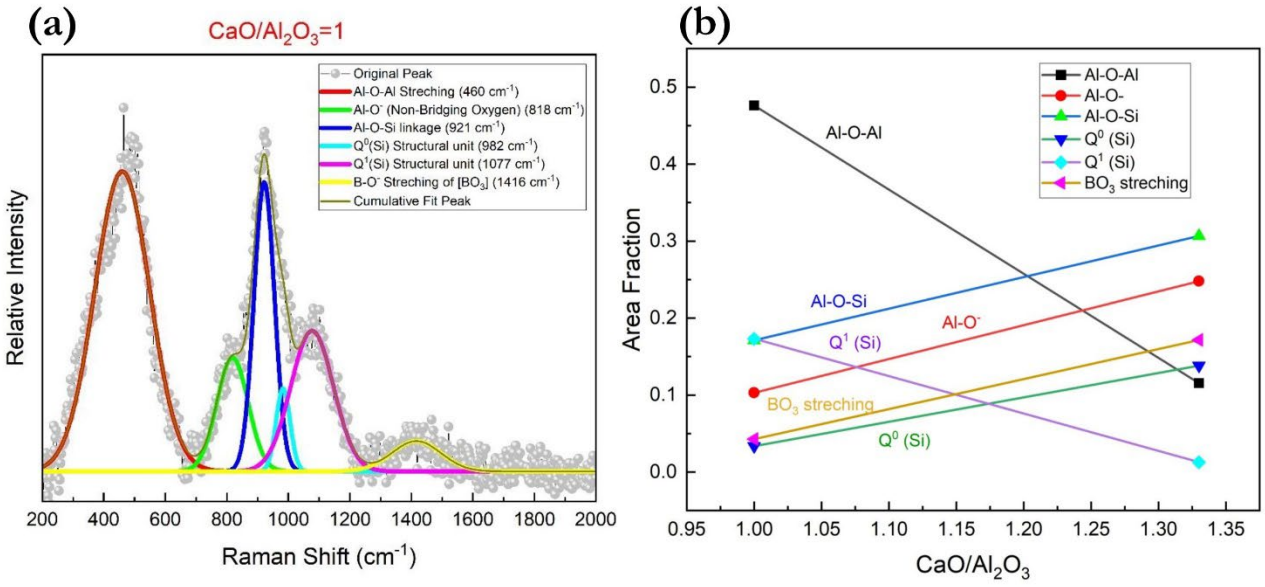

FIG 8– (a) Deconvoluted Raman Spectra of CaO/Al_2O_3=1.00,(b) Area fraction of various structural units present in the two compositions

The melt structure of calcium aluminate-based mold fluxes plays a crucial role in influencing both viscosity and crystallization tendencies. These factors, in turn, impact the lubrication and heat transfer capabilities of the mold fluxes to the steel shell. The structural role of Al_2O_3 in the melt structure is intricate due to its amphoteric nature. The slag system's constituents, which can act as network formers or breakers, depend on the type of steel being cast. Understanding the melt structure of the calcium aluminate slag system and how it evolves with the replacement of SiO_2 by Al_2O_3 has been the subject of numerous studies(Zhou *et al.*, 2021).

Figure 8(a) shows the deconvoluted Raman spectra for the CaO/Al_2O_3=1.00 glassy mold flux. The spectral pattern at approximately 460 cm^{-1} in the low-frequency range of the Raman spectra corresponds to the Al-O-Al stretching characteristics peak, indicative of the bridging oxygen in the aluminate network containing $[AlO4]^{5-}$ units. Within the mid-frequency range (700–1300 cm^{-1}), the spectra reveal the depolymerization of the aluminosilicate structure, signifying $Al\text{-}O^-$ or $Si\text{-}O^-$ telescopic vibrations. Specifically, the peaks at 818 cm^{-1} and 921 cm^{-1} represent the symmetric Al-O− and Al-O-Si bonds, respectively. The degree of polymerization or depolymerization is denoted by Q^n, where 'n' signifies the number of bridging oxygen units. Q^0 corresponds to $[AlO4]^{5-}$ or $[SiO4]^{4-}$ units, with structural units Q^0(Si) and Q^1(Si) identified by peaks at 982 cm^{-1} and 1077 cm^{-1}, respectively(Wahyudi, 2023).

$$[AlO_4]^{5-} + O^{2-} = [AlO_5]^{7-}$$

The peak at 1416 cm^{-1} is assigned to the symmetric stretching vibrations of terminal oxygen atoms in orthoborate units $[BO_3]$. This suggests that the predominant formation of $[BO_3]$ groups in the mold flux is indicative of B^{3+} involvement in the structure.

Figure 8 (b) shows that as $wt\%CaO/wt\%Al_2O_3$ increases from 1.00 to 1.33 the area fraction of Al-O-Al(bridging oxygen) and Q^1(Si) decreases while $Al\text{-}O^-$, Al-O-Si, Q^0(Si) and $[BO_3]$ increases, this indicates that more complex aluminate and silicate structure is transformed into the simpler one. As the $w(CaO)/w(Al_2O_3)$ increases weight fraction of CaO will increase, as there will be excess CaO the O^{2-} ions in the melt will depolymerize the chain. This indicates that higher CaO/Al_2O_3 ratios will decrease the viscosity of the melt as there will be more mobility of ions due to a higher number of non-bridging oxygen and this might also increase the crystallization tendency (Shao *et al.*, 2019).

CONCLUSIONS

The isothermal crystallization kinetics of two mold fluxes of different CaO/Al_2O_3 ratios were investigated systematically. Based on the kinetic parameters of the JMAK model the crystallization mode was determined. The main conclusions are summarized as follows.

1. The average value of the Avarami exponent n for the wt%CaO/wt%Al_2O_3 =1.00 is ~4 and for wt%CaO/wt%Al_2O_3 =1.33 is ~3.5 indicating the $C_{12}A_7$ crystal growth is 3 dimensional with constant nucleation rate.
2. The effective rate constant (k) for the formation of $C_{12}A_7$ in both mold flux compositions exhibits an increase as the crystallization temperature decreases. This indicates that elevated temperatures impede the overall crystallization rate, suggesting that the process is governed by nucleation across a range of crystallization temperatures.
3. The effective activation energy of $C_{12}A_7$ formation for the mold fluxes wt%CaO/wt%Al_2O_3 =1.00 and 1.33 is -102.75 KJ/mol and -69.72 KJ/mol respectively. The negative value of activation energy means that it is showing anti-Arrhenius behavior, indicating that crystallization is determined by nucleation.
4. As the wt%CaO/wt%Al_2O_3 ratio increased from 1.00 to 1.33 the peak crystallization temperature of the $C_{12}A_7$ phase decreased 915^{o}C to 800^{o}C.
5. The depolymerization of the various structural units because of the various network breakers led to the formation of simpler structural units by increasing NBO, which in turn will enhance the crystallization tendency of the melt as we increase the wt%CaO/wt%Al_2O_3 ratio from 1.00 to 1.33.

ACKNOWLEDGEMENTS

The author wishes to extend thanks to the multiple laboratories within the Department of Materials Science and Engineering at IIT Kanpur for generously providing the necessary facilities for the ongoing research.

REFERENCES

Avrami, M. (1939) ‘Kinetics of phase change. I: General theory’, *The Journal of Chemical Physics*, 7(12), pp. 1103–1112. doi: 10.1063/1.1750380.

Aydin, H. *et al.* (2013) ‘Development of 3rd generation AHSS with medium Mn content alloying compositions’, *Materials Science and Engineering A*, 564, pp. 501–508. doi: 10.1016/j.msea.2012.11.113.

Cho, J. W. *et al.* (2013) ‘Assessment of CaO-Al2O3 based mold flux system for high aluminum TRIP casting’, *ISIJ International*, 53(1), pp. 62–70. doi: 10.2355/isijinternational.53.62.

Kim, D. J. and Park, J. H. (2012) ‘Interfacial reaction between CaO-SiO 2-MgO-Al 2O 3 flux and Fe-xMn-yAl (x = 10 and 20 mass pct, y = 1, 3, and 6 mass pct) steel at 1873 K (1600 °c)’, *Metallurgical and Materials Transactions B: Process Metallurgy and Materials Processing Science*, 43(4), pp. 875–886. doi: 10.1007/s11663-012-9667-x.

Liu, Q. *et al.* (2014) ‘Development of mould fluxes based on lime-alumina slag system for casting high aluminium trip steel’, *Ironmaking and Steelmaking*, 41(4), pp. 292–297. doi: 10.1179/1743281213Y.0000000131.

Papageorgiou, G. Z. *et al.* (2005) ‘Crystallization kinetics and nucleation activity of filler in polypropylene/surface-treated SiO2 nanocomposites’, *Thermochimica Acta*, 427(1–2), pp. 117–128. doi: 10.1016/j.tca.2004.09.001.

Salasin, J. R. and Rawn, C. (2017) ‘Structure property relationships and cationic doping in [Ca24Al28O64]4+ framework: A review’, *Crystals*, 7(5). doi: 10.3390/cryst7050143.

Seo, M. D. *et al.* (2015) ‘Kinetics of Isothermal Melt Crystallization in CaO-SiO2-CaF2-Based Mold Fluxes’, *Metallurgical and Materials Transactions B: Process Metallurgy and Materials Processing Science*, 46(5), pp. 2374–2383. doi: 10.1007/s11663-015-0358-2.

Shao, H. *et al.* (2019) ‘Effect of fluorine and CaO/Al2O3 mass ratio on the viscosity and structure of CaO–Al2O3-based mold fluxes’, *Journal of the American Ceramic Society*, 102(8), pp. 4440–4449. doi: 10.1111/jace.16322.

Vyazovkin, S. and Sbirrazzuoli, N. (2003) ‘(-) (4)’, (6), pp. 882–888.

Wahyudi, R. (2023) ‘Metadata of the chapter that will be visualized in Online’, *Springer Nature Singapor*, (August), pp. 1–8.

Zhang, L., Wang, W. lin and Shao, H. qing (2019) ‘Review of non-reactive CaO–Al2O3-based mold fluxes for casting high-aluminum steel’, *Journal of Iron and Steel Research International*, 26(4), pp. 336–344. doi: 10.1007/s42243-018-00226-2.

Zhou, L. *et al.* (2021) ‘Crystallization behavior and melt structure of typical CaO–SiO2 and CaO–Al2O3-Based mold fluxes’, *Ceramics International*, 47(8), pp. 10940–10949. doi: 10.1016/j.ceramint.2020.12.213.